DOI: 10.22034/ijicmes.2026.564348.1006

University of Hormozgan

International Journal of
Innovative Computational Methods
in Engineering Sciences
*2026, * (*), *-***
journal homepage – cme.hormozgan.ac.ir

Optimal MV overhead line arrangement for improvement of the shear-accelerated aging of the H-type concrete power poles

Meisam Pourahmadi-Nakhli[a,*], Hamid Reza Firouzabadi[b], Abbas Harifi[a]

[a] *Department of Electrical and Computer Eng., University of Hormozgan, BandarAbbas, Iran*
[b] *Hormozgan Electric Distribution Company (HEDC), BandarAbbas, Iran*

ARTICLE INFO

***Keywords**:*
FEM
Concrete power poles
wind force
overhead line arrangements
pole backfill

Received:
Revised:
Accepted:
Available online

ABSTRACT

Functionally graded materials (FGMs) have a heterogeneous and advanced structure, Experience and evidence show that power poles installed in provinces around the Persian Gulf are more prone to premature concrete failure. Specifically, severe concrete fractures and cracks occur around the pole anchor due to reduced elasticity, which increases porosity and accelerates the attack of chemical agents. In this study, various factors contributing to wind-induced shear at the anchor are investigated using the Finite Element Method (FEM). On this basis, the optimal power line arrangement and pole installation are proposed in comparison with the available standards and procedures in Iran. Using the FEM analysis tools PLS-Pole and Abaqus, the stress induced by wind force is investigated for different available scenarios of medium voltage (MV) overhead line designs. Results show that the effects of conventional power pole implementations and arrangements on pole fatigue have been neglected in design. From this viewpoint, standards in Hormozgan need to be dramatically changed to reduce wind-driven stress by up to 40%. Having negligible influences on other power line performances, these changes include the use of suspension insulators instead of pin insulators, 1.5 m instead of 2 or 2.44 m crossarms, 12 m or even 9 m instead of 15 or 14 m poles, 400 kgf instead of 600 kgf poles, 40 m instead of 50 or 60 m line spans, one instead of two overhead circuits, and soil backfill instead of concrete backfill.

1. Introduction

Most of the medium voltage power networks in Iran are overhead lines resting on concrete cantilever poles. This is due to the fact that the development of the underground MV networks in suburbs and sometimes in urban regions are not economically or technically justifiable. One of the most evident symptoms of concrete power pole failures on the coastal overhead lines of the Persian Gulf is cracking or spalling of the concrete at the anchor point above the buried part. To date, the common belief has been that high penetration of sulfate and chloride salts from the Persian Gulf is to blame; thus, power system operators have made a great deal of effort to tackle these corrosive agents in the first place [1-3]. It includes preventative measures from improving the concrete mix to the use of the preventive sealers and coatings. Despite huge investments to implement these measures, concrete power poles in the southern coastal provinces of Iran suffer a short lifetime, and in some cases, the poles need to be replaced after only five years. Some other researchers have

* Corresponding Author: m.pourahmadi@hormozgan.ac.ir

investigated the effects of stray currents induced or leaked from conductors on aging of the concrete power poles [4]. However, the symptoms of damage are so extensive and critical on the MV network of HEDC that the effect of stray currents is considered minimal in comparison.

Fig. 1. Anchor damage due to accelerated corrosion

However, the characteristics of the common damage to HEDC power poles are distinctive, as it occurs at the anchor point where mechanical stresses are maximum. This specific behavior underlines the influences of the concrete tension on the rate of chemical corrosion.

Some researchers investigated the durability of the power poles or other cantilever concrete beams under mechanical forces [5-9]. However, only a few paid attentions on the link between the rate of chemical corrosion and mechanical fatigue of the poles. In this study, the effects of the wind induced moment on power pole corrosion are investigated and different contributing factors on minimizing of this force are examined to obtain an optimal pole arrangement. Recent studies have further reinforced the link between mechanical stress and accelerated corrosion in concrete infrastructure. Brown et al. [12] demonstrated through finite-element analysis and centrifuge modeling that backfill density and foundation shape significantly influence uplift capacity, with optimized backfilling enhancing tensile capacity by up to 40%. Song et al. [13] showed that concrete cracking accelerates rebar corrosion rates by 2.5–3.4 times under combined chloride and sulfate attack, highlighting the critical positive feedback between mechanical damage and chemical degradation. Amouri and Fawzi [11] provided mechanistic insights into sulfate–chloride co-exposure resistance, emphasizing the importance of reducing mechanical stress in corrosive environments. Furthermore, the updated IEC 61109:2025 standard [10] provides revised test methods and acceptance criteria for composite suspension insulators, supporting our recommendation to adopt suspension insulators over pin-type insulators in coastal regions

The motivation for this study stems from a critical but overlooked observation in the coastal regions of Iran: despite significant investments in chemical countermeasures—such as improved concrete mixes, sealers, and coatings—concrete power poles continue to fail prematurely at the anchor point. This persistent issue suggests that mechanical stress, rather than chemical attack alone, plays a major accelerating role in concrete deterioration, a factor largely neglected in both national standards and existing literature. The novelty of this study lies in: (1) systematically isolating the contribution of multiple design parameters—including pole length, crossarm length, insulator type, span length, backfill type, pole strength, circuit arrangement, and number of circuits—to wind-induced anchor stress; (2) providing, for the first time for the

Persian Gulf region, a quantitative sensitivity analysis of these factors using validated FEM simulations (PLS-Pole and Abaqus); and (3) proposing specific, actionable modifications to Iranian national standards that collectively reduce anchor stress by up to 40% with minimal cost implications, thereby extending pole service life in corrosive environments.

2. Observation

An extensive survey was made by authors in Hormozgan Electric Distribution Grid to investigate different factors on pole aging. Observations confirmed that poles far from the coast experience fewer concrete and armor failures for an obvious reason: the concentration of sulfate and chloride decreases from the coast inland.

Regardless of this fact, evidence shows a significant link between the level of corrosion and the level of concrete exposure to wind force under the same climatic conditions. Consequently, power poles with anchors exposed to higher forces experience shorter lifetimes, with critical cracks and damage in the concrete. Three observations from three parallel laterals of the Armak MV overhead circuit in Bandar Charak (Charak Port), Hormozgan, Iran, are presented as follows:

Observation #1: Figure 2 shows two representative poles of the lateral to Armak Mill, developed in 1997. The circuit arrangement of the Armak Mill lateral carries three Hyena conductors bonded to three pin insulators fixed on a 2.44 m crossarm, with 12 m poles directly mounted and fixed with concrete backfill (inelastic foundation). Most poles in this lateral suffer severe concrete destruction at the anchor.

Fig. 2. Severe damage at pole anchors of Armak 'mill lateral (support insulators, concrete backfill, 1997)

Observation #2: Elsewhere on the Armak main line, parallel to the Armak Mill lateral (with the same wind exposure), there is a lateral developed in 1991. Poles of this lateral were initially installed to carry three Hyena conductors bonded to three pin insulators fixed on a 2 m crossarm, with 12 m poles directly mounted and fixed with concrete backfill (inelastic foundation). Later, in 1997, the two pin porcelain insulators at the wings were replaced with rubber suspension insulators. Observations confirm moderate anchor damage compared to that of the Mill lateral. Figure 3 indicates two representative poles of the 1991-developed part of the Armak main.

Fig. 3. Moderate damage at pole anchors of Armak main (suspention insulators, concrete backfill, 1991)

Observation #3: Interestingly, in the same region with the same wind exposure, poles of the Armak-Charak main line developed in 1994 are now in good condition with no visible cracks at the anchor (see Figure 4). Similar to the 1991-developed section of the Armak-Charak main line, the poles of this lateral carry three Hyena conductors bonded to one pin insulator at the pole tip and two suspension insulators at the wings of a 2 m crossarm. The major difference is that the 12 m poles are directly mounted and fixed with compacted soil (a more elastic foundation than concrete).

Fig. 4. No visible damage at pole anchors of Armak-Charak main (suspention insulators, soil backfill, 1994)

3. Materials

Table 1 presents standard arrangements of the medium voltage overhead line on H-type armored concrete power poles commonly used in HEDC. All of the scenarios indicated in the first column of the table are Pole Codes (PC) presented in Appendix 1. Standard Pole Lengths (PL) are 15, 14 and 12 meters each of which have Berrial Length (BL) of 2.1, 2, and 1.8 meters when mounted directly. NoC, in 4th column, indicates number of conductors. Circuit Arrangement (CA) in 5th column can be double-sided, L, tangential, flag and cross types with Arm Length of 1.5, 2 and 2.44 (m) in column 6th (also see appendix 1). Insulator Type (IT) can be a suspension (hanged) and/or pin (fix) types. Span Length (SL) can be 40 or 50 m with Foundation Module of Elasticity (FME) of inelastic concrete backfill (rigid) or soil backfill with elasticity of the 10000(ksi). According to the last column, Pole Strength (PS) can withstand 400 or 600 kgF. Other details of the pole arrangements including pole dimensions, conductor and crossarm locations are presented in appendix I.

4. Calculations

4.1. Equivalent wind force on power poles

Wind force tolerance is the major factor in determining pole strength (kgf). The equivalent wind force exerted on the pole depends on the wind speed, pole surface, diameter and number of conductors and the spa[illegible] wo poles. Wind force per meter of a conductor of diameter *d* (mm) is:

$$W_w = [illegible] d \times 10^{-3} \quad (1)$$

[illegible] F_w is wind pressure at wind speed V(m/s):

$$F_w = \frac{[illegible]}{16[illegible]} \quad (2)$$

[illegible] equivalent wind force (kgF) on a pole supporting N conductors with span S_w(m) is:

$$W_H = NS_w(\rho W_w) \quad (3)$$

Table . 1. Line arrangement parameters

PC	**PL**(m)	**BL**(m)	**NoC**	**CA**	**AL**(m)	**IT**	**SL**(m)	**FME**(ksi)	**PS**(kgf)
A-I	15	2.1	6	2-side	2m	Sup	50	Rigid	600
A-II	15	2.1	6	2-side	2m	Sus	50	Rigid	600
A-III	15	2.1	6	2-side	1.5m	Sus	50	Rigid	600
A-IV	15	2.1	6	2-side	1.5m	Sus	40	Rigid	600
A-V	15	2.1	6	2-side	1.5m	Sus	40	10000	600
A-VI	15	2.1	6	2-side	1.5m	Sus	40	10000	400
B-I	14	2	6	2-side	2m	Sup	50	Rigid	600
B-II	14	2	6	2-side	2m	Sus	50	Rigid	600
B-III	14	2	6	2-side	1.5m	Sus	50	Rigid	600
B-IV	14	2	6	2-side	1.5m	Sus	40	Rigid	600
B-V	14	2	6	2-side	1.5m	Sus	40	10000	600
B-VI	14	2	6	2-side	1.5m	Sus	40	10000	400
C-I	12	1.8	6	2-side	2m	Sup	50	Rigid	600
C-II	12	1.8	6	2-side	2m	Sus	50	Rigid	600
C-III	12	1.8	6	2-side	1.5m	Sus	50	Rigid	600
C-IV	12	1.8	6	2-side	1.5m	Sus	40	Rigid	600
C-V	12	1.8	6	2-side	1.5m	Sus	40	10000	600
C-VI	12	1.8	6	2-side	1.5m	Sus	40	10000	400
D-I	12	1.8	3	L-type	2m	Sup	50	Rigid	600
E-I	12	1.8	3	Tang.	2.44m	Sup	50	Rigid	600
F-I	12	1.8	3	Flag	0.6m	Sup	50	Rigid	600
G-I	12	1.8	3	Cross	2m	Sup	50	Rigid	600
G-II	12	1.8	3	Cross	1.5m	Sup	50	Rigid	600
G-III	12	1.8	3	Cross	1.5m	Sus	50	Rigid	600
G-IV	12	1.8	3	Cross	1.5m	Sus	40	Rigid	600
G-V	12	1.8	3	Cross	1.5m	Sus	40	10000	600
G-VI	12	1.8	3	Cross	1.5m	Sus	40	10000	400

Where ρ is the coe[illegible]nt depending wind flactuations, sea-level height and wind incident angle. When all are unknown then $\rho = 1$.

The vertical force of the conductor's mass W_c(kg/m) of this span is:

$$W_v = N S_w W_c \tag{4}$$

4.2. *Wind-induced tension calculations on the pole axis*

PLS-Pole software is applied to numerically calculate the transverse moment and shear exerted on the pole axis due to wind. The Hyena conductors of d=14.57 mm and $W_c = 0.45$(kg/m), and the exposure to a maximum horizontal wind speed of 20 m/s with $\rho = 1$ are considered.

As noted, before, mechanical and shear stresses can add to porosity and cracks of the concrete. Moreover, since the anchor region of the pole is mostly exposed to periodic penetration of the corrosive agents of chloride and sulfate, demonstration of the results is confined to the region above anchor e.g., from ground level up to 60cm; evidence confirms that most critical concrete fractures and collapses, and other minor corrosion symptoms like cracks and formation of white and brown patches are noticeable in heights less than 60cm.

Figures 5 show the color-distribution of the transverse shear (kips) along the desired segment of the poles. Figure 5 presents the distribution of wind shear at different sections up to 60 cm above ground level under a wind speed of 20 m/s on the pole face and Hyena conductors. In this figure, scenarios are illustrated in a specific order that the changes in the parameters result in continues decrease in the transverse moment. The first, the second and the third rows of plots indicate the wind-caused stress respectively for poles of 15, 14 and 12 meters carrying 6 conductors

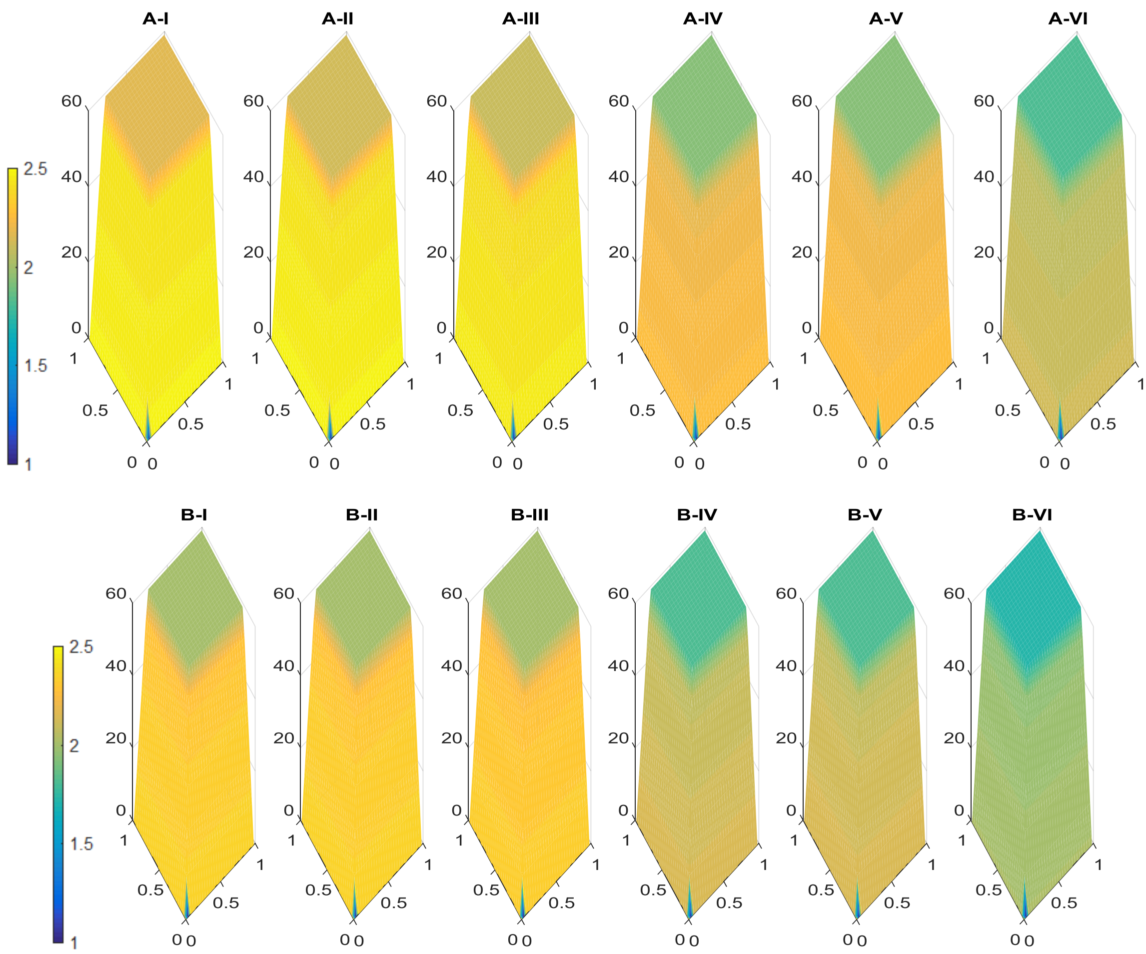

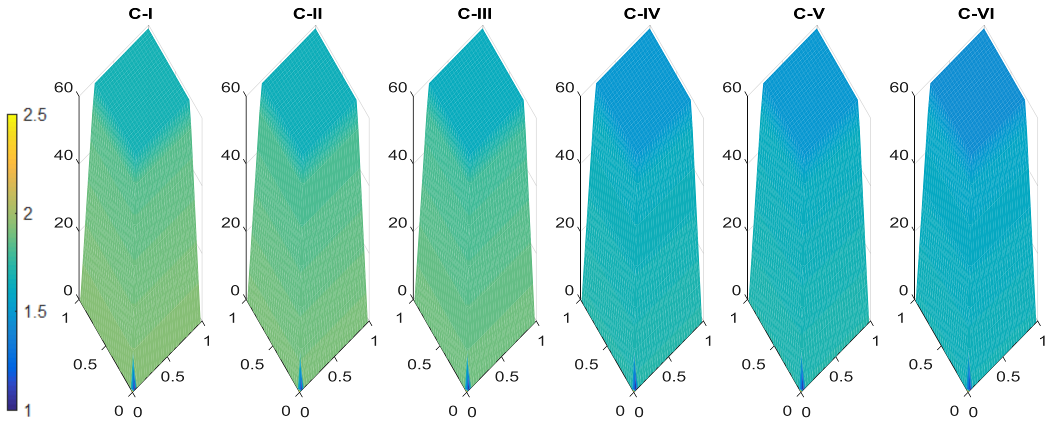

Fig. 5. Color – distribution of the trans. Shear (kips) for poles supporting 6 conductors

The results of figure 5 significantly prove that under the same conditions but with the reduction of the pole lengths from 15 to 12 meters, the amount of torque stress and tangential shear force on the axis of the base are significantly reduced. It also indicates that the maximum tension occurs at the ground level (upper anchor) and decreases with the reduction of the length of the pole in the corresponding arrangements. This reduction in torque and tangential shear force is achieved due to the reduction in the length of the torque lever (by reducing the height of the base or by displacement of the crossarm to lower holes). The color-bars confirm that the changes towards shorter crossarms, suspension insulators, shorter spans, more elastic foundations and also reducing the pole strength will have a direct effect on reducing the transferred force to the pole axis.

It is worth noting that with the decrease of the pole strength, the total volume and as a result, the weight of the pole is reduced. In explaining this relationship, it should be noted that in each of the arrangements, the center of gravity of the base deviates from the vertical axis by wind force because of the elasticity of the armored pole. On the other hand, the deviation of the center of gravity adds to the tangential force all over the pole. That is to say the stronger the pole, the heavier it is, and as a result, this can lead to further increase in tangential stress for 600 kgf poles (A, B and C-V) compared to 400 kgf poles (A, B and C-VI).

Figure 6 represents the values of transverse torque of figure 5 exactly at ground level points. These trends can also be generalized to other points above. Table 2 shows the percentage of stress reduction per changes with respect to the references of A, B and C-I codes. As mentioned earlier, this significant reduction in the amount of tangential force to the base axis is due to the reduction of the cross-arm length, hanged instead of fixed insulators, larger elastic backfills (for example soil instead of concrete backfills), the reduction of the span length and the reduction of the strength of the poles from 600 kgf to 400 kgf.

Consider ABC-I poles of 15, 14 and 12 m each of which having 600 kgf strength, with fixed anchor (inelastic concrete foundation), with pin insulators fixed on 2-meter cross arms and 50-meter span as references. Changes are compared to these references. According to Table 2, by changing A-I arrangement to 15m-400 kgf strength poles, 6 suspension insulators supported on 1.5 m crossarms in the 40 m span and without concreting the foundation, it is possible to achieve more than 17.27% reduction in the torque and 14.22% in the tangential shear at anchor. The reductions of the moment and the shear for B-I and C-I are rather the same as A-I.

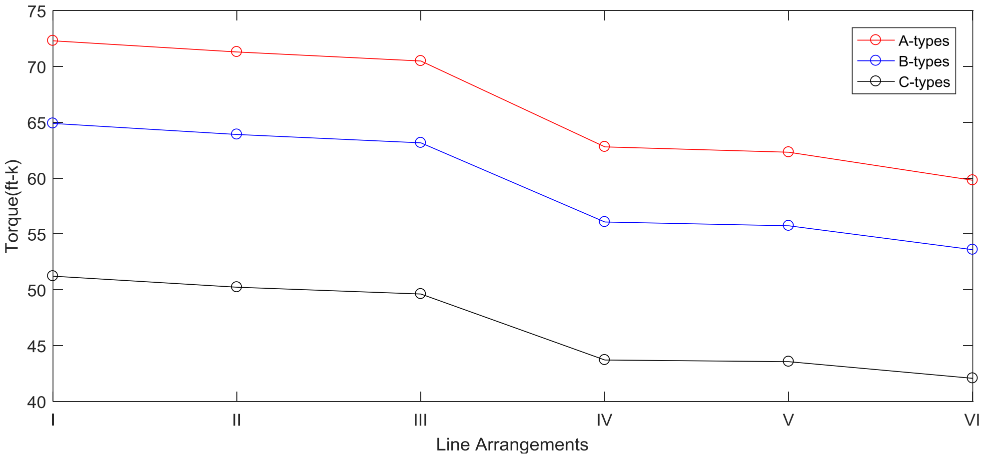

Fig. 6. Transverse moment (ft-k) at anchor point of A,B and C-type poles

From table 2 one can also argue that a significant reduction of 40% in the transferred moment and 26% in the transferred shear are achievable when 15 m reference arrangement (A-I) is changed to the 12 m arrangement of C-VI. This important finding regarding the significant reduction of the tension can address the following questions in the implementation of the distribution networks of Hormozgan province: first, to deregulate the considerations and restrictions of line clearance at least for coastal MV networks of the Persian Gulf. Second, like many countries that use shorter concrete poles for power delivery in the MV network, to employ 12 m poles instead of 15 m poles where safety measures allow (acceptable line clearance). By these deregulations at least in coastal provinces, where are prone to corrosion, the mechanical stress as a major corrosion-accelerating factor can be mitigated.

Table 2. Percentage change of the tentions at anchor point w.r.t. benchmarks

Tension type	**A-II**	**A-III**	**A-IV**	**A-V**	**A-VI**
Trans. Torque	-1.38%	-2.50%	-13.13%	-13.80%	-17.27%
Trans. Shear	0%	-0.813%	-8.53%	-8.13%	-14.22%
Tension type	**B-II**	**B-III**	**B-IV**	**B-V**	**B-VI**
Trans. Torque	-1.52%	-2.68%	-13.60%	-14.12%	-17.42%
Trans. Shear	0%	-0.85%	-8.93%	-8.93%	-14.46%
Tension type	**C-II**	**C-III**	**C-IV**	**C-V**	**C-VI**
Trans. Torque	-1.93%	-3.12%	-14.66%	-14.95%	-17.86%
Trans. Shear	0%	-0.93%	-9.85%	-9.85%	-14.55%

Figures 7 (a), (b) and (c) illustrate the displacement of these elastic concrete poles in the range of 60 cm above the ground, respectively for 15, 14 and 12-meter arrangements. As shown, by increasing the modulus of elasticity of the foundations in codes A, B and C-V and A, B and C -VI, they experience a larger displacement. In practice, higher elastic foundation is viable by backfilling the buried part with soil instead of concrete.

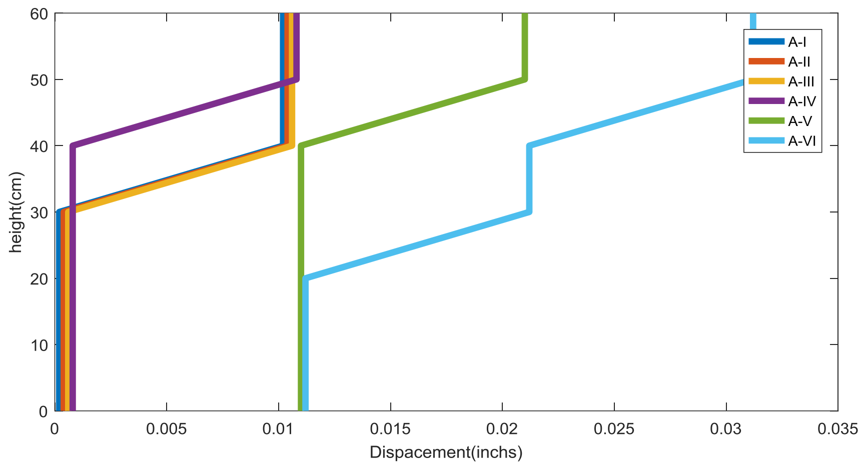

(a)

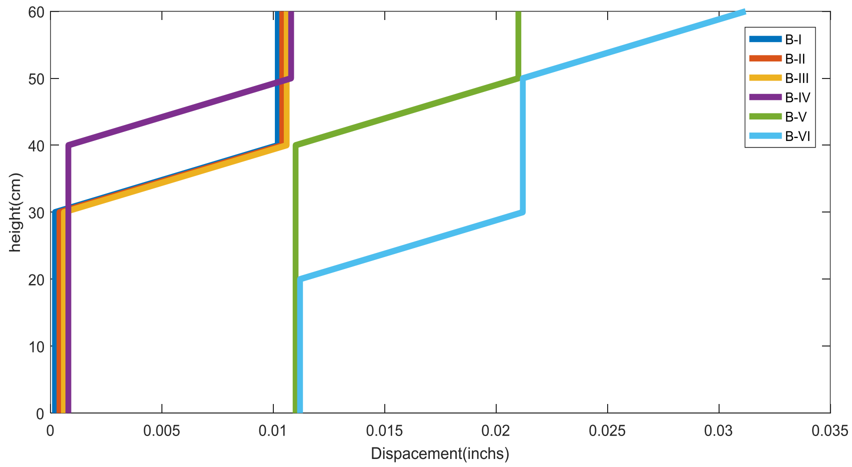

(b)

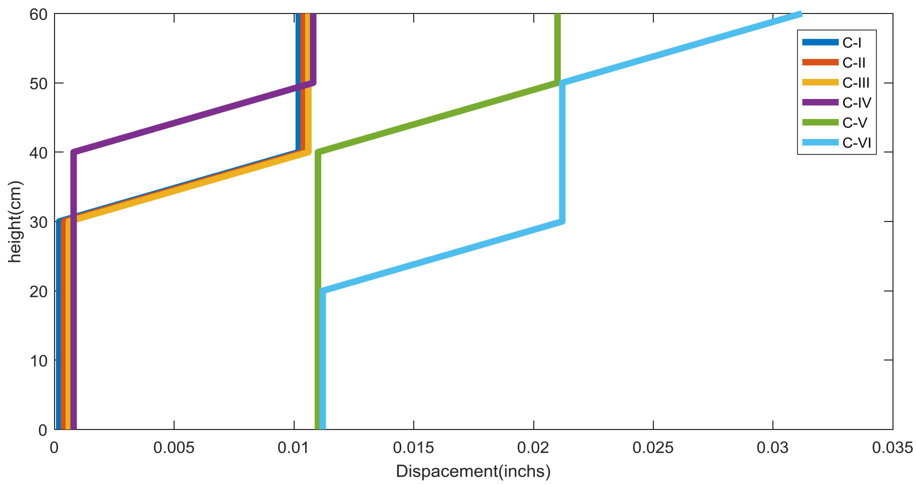

(c)

Fig. 7. Displacement over 60 cm from ground level: (a) A-type poles, (b) B-type poles over 60 cm, (c) C-type poles

Here simulations are done for pole arrangements of 12m carrying 3 conductors (one 3-phase circuit), and the effective factors for mitigating the stress on the common 12m MV arrangements carrying 3 conductors in HEDC are examined. Figure 8 shows the distribution of wind stress in terms of transverse shear (kips) along the section above the ground up to 60 cm of arrangements D-I, E-I, F-I, G-I to G-VI. This tangential force is induced by wind speed of 20 m/s on 3 Hyena conductors. Table 3 and Figure 9 present the variation of the anchor moment at ground level points of D to G-VI arrangements. Considering D-I arrangement with L-arm supporting 3 pin conductors as reference (see appendix 1), one can achieve 19.48% reduction in the tangential moment and 15.18% in the shear stress by applying the following changes in 12m pole arrangements: the L-arm/12m-600kgf/pin-insulator/concrete foundation/ 50m span replaced with a cross-arm/12m-400kgf/ wing-suspension insulators/soil backfill/40m span (see table 3). Wind-induced displacement of the 12 m poles are also evident in figure 10 for different arrangements.

Table 3. Percentage change of the tentions at anchor point w.r.t. benchmark

Tension type	E-I	F-I	G-I	G-II	G-III	G-IV	G-V	G-VI
Trans. Torque	-3.47	-5.01	-6.1	-7.39	-5.65	-14.78	-15.25	-19.48
Trans. Shear	-1.89	-0.63	-1.89	-2.53	-2.53	-8.86	-8.86	-15.18

From the results of the figures and tables of all simulations, it can be concluded that shortening the arm, lowering the crossarm (shorter pole), suspending the insulator, reducing the length of the span, reducing the strength of the pole (weight of the concrete structure) and increasing the elasticity of concrete have direct effects on reducing the stress at anchor.

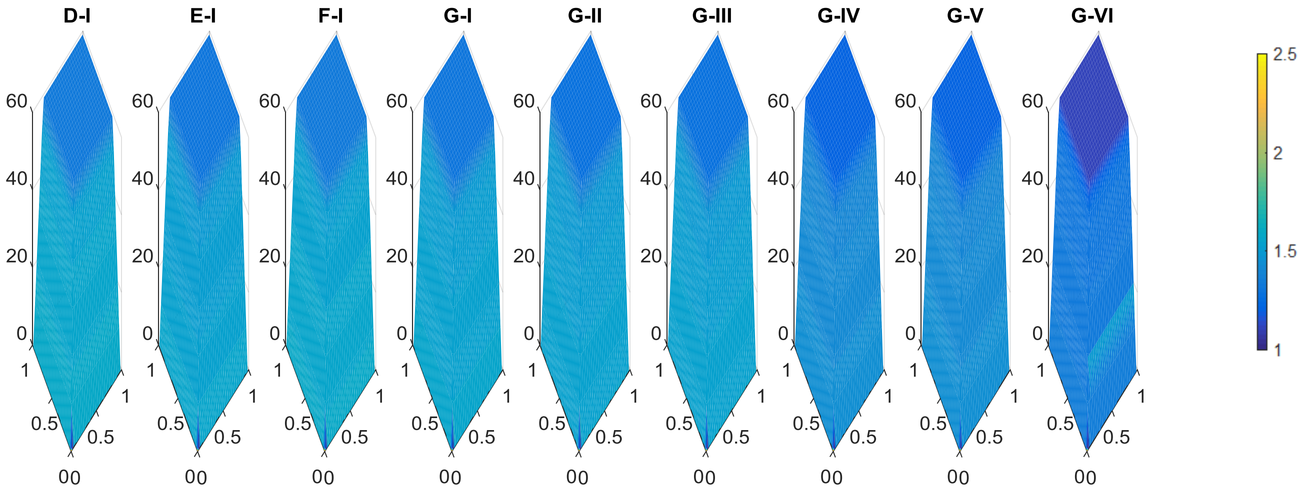

Fig. 8. Color – distribution of the trans. Shear (kips) for poles supporting 3 conductors

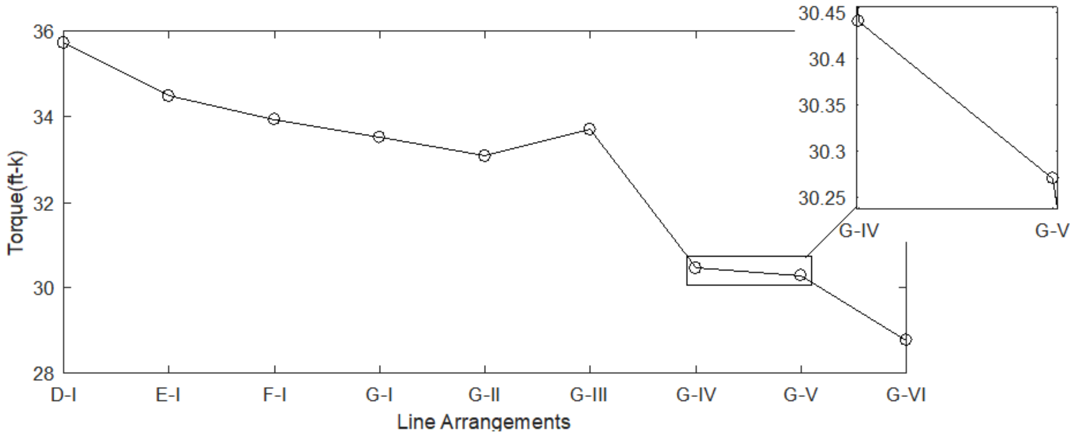

Fig. 9. trans. Moment (ft-k) at anchor point of D, E, F and G-type poles

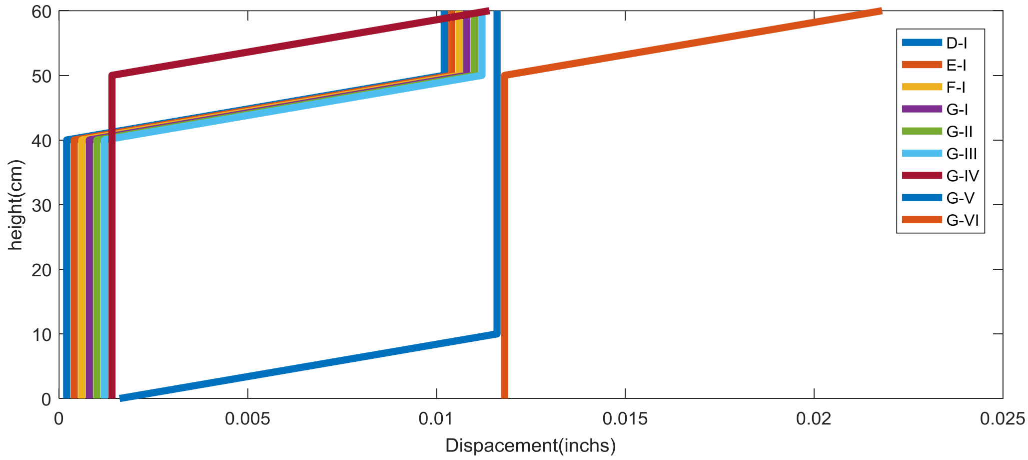

Fig. 10. Displacement of E, F and G-type poles over 60 cm from ground level

5. Backfill effect

Field investigation revealed that poles supported by soil backfill have fewer cracks and less anchor damage compared to poles fixed in concrete backfill. This suggests that elasticity of the backfill around the buried part of the poles can influence the distribution of tension at anchor. The two most common methods of backfilling for directly embedded poles are the use of soil backfill and concrete backfill. Nowadays in Iran, it is a common practice to use 400-grade concrete as a filler around the rocks holding the pole. Concrete backfill is deemed to increase the stability of the foundation. However, in many cases at initial pole installation which is done by rocks and soil backfill, the rocks provide enough pole position stability and there is no need for concrete. For example, in the case of timber poles, soil backfill provides a stable foundation, and where necessary, guy-wires are employed to fix the pole position without concreting.

Regardless of pole stability, an inelastic backfill (non-armored concrete backfill) does not allow tangential displacement of the buried part, resulting in a rigid anchor. From this point of view, the moment caused by wind forces are exerted stronger and thus more destructive to the ground level concrete. Although field evidence supports this heuristic justification, FEA (Finite Element Analysis) simulation using Abaqus was employed to simulate the condition. This is to compare between the effect of non-armored (rigid) concrete backfill with the modulus of elasticity of 1000 ksi and soil backfill with the modulus of elasticity of 10000 ksi.

A detailed simulation of a 12m-400kgf concrete pole is conducted in Abaqus software with applying a 274 kg tangential force at 60 cm from the tip. The color bar results of a rigid concrete foundation and an elastic concrete foundation (near the elasticity of compact rock-soil) are shown in Figure 11 (a) and (b), respectively. This simulation confirms the increase of force up to 5.32 kN at the anchor point (ground level) in concrete base with elasticity of 1000ksi. Furthermore, simulation results of the same pole and input force with foundation elasticity of 10000ksi was conducted. This simulation confirms the force reduction at the same point to 4.64 kN. The amount of stress transferred to the ground level for soil backfill dropped by about 12% (refer to Figure 11(b)).

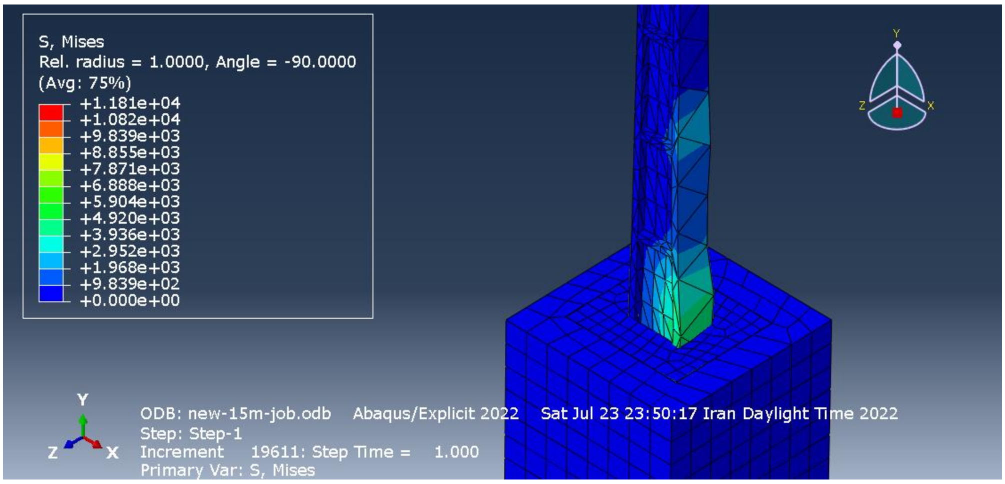

(a)

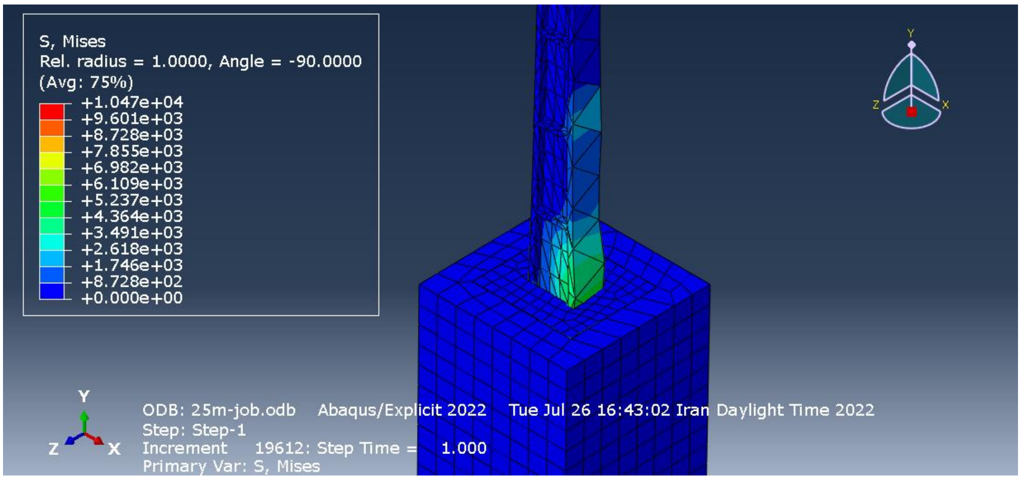

(b)

Fig. 11. Force distribution in newtons on concrete base placed in concrete with: (a) elasticity of 10000 (ksi) (b) elasticity of 1000 (ksi)

6. Sensitivity analysis

To isolate the individual contribution of each design factor to anchor stress reduction, a sensitivity analysis was performed using FEM results from PLS-Pole and Abaqus, with marginal reductions in transverse torque and shear quantified for each parameter (summarized in Table 4). The results reveal that span length reduction (50 m → 40 m) is the most dominant individual factor, achieving an 11.5–13.6% torque reduction and 8.5–9.9% shear reduction by directly decreasing wind load on conductors. Pole length reduction (15 m

→ 12 m) provides the largest cumulative impact (17.9–19.5% torque, 14.6–15.2% shear), challenging Iran's conventional preference for taller poles and supporting deregulation of clearance constraints in coastal corrosive environments. Backfill type shows only a 0.3–0.7% marginal torque reduction in PLS-Pole analysis but a substantial 12.8% force reduction in Abaqus simulations (5.32 kN to 4.64 kN), with soil backfill offering critical long-term fatigue benefits through elastic deformation—consistent with field Observation #3, where soil-backfilled poles showed no visible damage after decades. Pole strength reduction (600 kgf → 400 kgf) contributes 2.9–3.5% torque and 5.7–6.3% shear reduction due to lower self-weight, while insulator type (pin → suspension) and crossarm length (2.0 m → 1.5 m) provide modest but consistent reductions of 1.4–1.9% and 1.2–1.5%, respectively—low-cost modifications readily adoptable in standards.

Furthermore, reducing the number of circuits (6 conductors → 3 conductors) achieves approximately 19% torque reduction by halving wind load, though this is operationally constrained by power demand. Symmetric circuit arrangements (cross-type) outperform asymmetric L-type, flag, or tangential configurations by 3.5–7.4% in torque reduction due to balanced force distribution. The combined optimal arrangement (e.g., C-VI or G-VI) yields a total torque reduction of 18–20% and shear reduction of 14–15% relative to current standard designs, demonstrating that while each factor contributes incrementally, their synergistic effect is substantially greater than any single modification alone. In summary, span length and pole length are the most impactful parameters for anchor stress reduction, while backfill type offers critical fatigue benefits beyond static torque analysis. For practical implementation in corrosive coastal regions such as Hormozgan province, the optimal design comprises shorter poles (12 m), shorter spans (40 m), soil backfill, suspension insulators, symmetric cross-arms, and 400 kgf pole strength.

Table 4. Sensitivity analysis of individual design factors on anchor stress reduction

Design factor	Parameter change	Effect on transverse torque	Effect on transverse shear	Remarks
Insulator type	Pin → Suspension	−1.38% to −1.93%	~0% to −0.93%	Minor to moderate reduction; suspension insulators allow slight movement, reducing moment transfer
Crossarm length	2.0 m → 1.5 m	−1.19% to −1.52%	−0.81% to −0.93%	Small but consistent reduction; shorter lever arm reduces bending moment
Span length	50 m → 40 m	−11.54% to −13.60%	−8.53% to −9.85%	Most dominant factor; directly reduces wind load on conductors
Backfill type	Concrete (rigid) → Soil (elastic)	−0.29% to −0.67%	~0% to −8.93% (shear)	Marginal torque reduction but significant force reduction (~12.8% from Abaqus) and improved fatigue behavior
Pole strength	600 kgf → 400 kgf	−2.91% to −3.47%	−5.69% to −6.33%	Lighter poles reduce self-weight moment and anchor stress
Pole length	15 m → 12 m	−17.86% to −19.48% (cumulative)	−14.55% to −15.18% (cumulative)	Major reduction; shorter lever arm significantly lowers anchor moment
Number of circuits	6 conductors → 3 conductors	−19.48% (D-I vs. G-VI)	−15.18% (D-I vs. G-VI)	Reducing conductor number halves wind load; very effective

Circuit arrangement	L-type / Flag / Tangential → Cross (symmetric)	–3.47% to –7.39% (from D-I to G-I/G-II)	–1.89% to –2.53%	Symmetric arrangements balance forces, reducing net moment
Combined optimal changes	Reference (C-I) → Optimal (C-VI or G-VI)	–17.86% to –19.48%	–14.55% to –15.18%	Maximum benefit achieved by simultaneously applying all recommended changes

7. Discussion

The significant reduction of anchor tension achieved by using 12 m two-circuit poles instead of 15 m and 14 m two-circuit poles requires deregulation of clearance (wire-to-ground distance) constraints in Iran. That is to say, unlike many countries where 12 m, 10 m, and even 9 m poles are permitted for medium voltage power delivery, the safer clearance provided by 14 m and 15 m poles has discouraged the widespread use of shorter poles in Iran for carrying six conductors. This clearance constraint has been the dominant practice so that power system operators in Iran barely use 12m 2-circuit poles even for supporting conductors having XLPE sheath. However, in many circumstances 15 m and 14 m poles are overdesigned options for safety plannings.

On one hand, 15 m and 14 m poles often provide safer clearance for medium voltage two-circuit lines (six-conductor lines). On the other hand, the risk of tension-accelerated corrosion and its associated costs are catastrophic. Yet in most of the cases, both constraints of safe clearance and tension reduction can be satisfied by use of 12m pole instead of 15 and 15 m poles. By weighing both sides, the high cost tips the scale in favor of short concrete poles, at least for regions with high exposure to corrosive agents.

Regarding the validation of the FEM models (PLS-Pole and Abaqus) used in this study, direct comparison with field observations served as the primary benchmark. Observations #1, #2, and #3 presented in Section 2 represent distinct combinations of the key contributing factors examined—pole length, insulator type, crossarm length, backfill material, and span length. The FEM simulations successfully reproduced the relative severity of anchor damage observed in practice: highest predicted shear stresses correspond to the severe damage of Observation #1 (pin insulators, concrete backfill, long crossarm), intermediate stresses match the moderate damage of Observation #2 (suspension insulators, concrete backfill), and lowest stresses align with the no-damage condition of Observation #3 (suspension insulators, soil backfill). This consistency confirms the predictive accuracy of the FEM models in capturing the mechanical behavior at the critical anchor zone.

With respect to the causality between reduced wind shear and decelerated chemical corrosion, while a precisely quantified corrosion rate would require long-term experimental studies, the three field observations establish this relationship convincingly when considered alongside fundamental material science principles. Observations #1, #2, and #3 were selected from parallel laterals under nearly identical environmental conditions (humidity, temperature, and concentration of corrosive agents such as sulfate and chloride), with the only significant differences being the mechanical stress factors. Poles exposed to lower wind-induced shear (Observation #3) showed no visible corrosion damage after decades, whereas those under higher shear (Observations #1 and #2) exhibited severe and moderate damage, respectively. This is consistent with the well-established mechanism that mechanical shear accelerates corrosion by inducing micro-cracking and macro-cracking in the concrete matrix, creating preferential pathways for chloride and sulfate ions to penetrate deeper into the concrete and reach the steel reinforcement. Once initiated, corrosion products expand, generating additional tensile stresses that exacerbate existing cracks—a positive feedback loop that further accelerates deterioration.

Regarding the material differences between 400 kgf and 600 kgf poles, it should be clarified that they share identical concrete mix design and material composition. Their difference in strength arises solely from larger cross-sectional dimensions and increased reinforcement volume in the 600 kgf poles. Consequently, the 600 kgf poles present a larger surface area to wind loading, generating higher resultant forces, and their greater mass and stiffness reduce foundation elasticity, leading to increased stress concentration at the anchor under equivalent wind conditions. Thus, the observed corrosion-fatigue advantage of the 400 kgf poles stems not from superior material durability but from reduced mechanical stress—which is precisely the focus of our proposed design modifications.

The economic impact of the proposed changes is noteworthy. Most of the proposed design modifications—including shorter poles (12 m instead of 15 m), soil backfill instead of concrete backfill, and symmetric conductor mounting—are either cost-neutral or cheaper than current practices. The only exception is the replacement of pin insulators with suspension insulators, which incurs a marginal additional cost. Regarding span length, reducing the span from 50 m to 40 m increases the number of poles by approximately 25%, raising initial infrastructure costs. However, this modification alone achieves a 17.27% reduction in anchor torque and a 14.22% reduction in tangential shear. This significant mechanical stress reduction directly extends the pole service life, substantially lowering long-term maintenance and replacement costs—particularly in the corrosive coastal environment. A preliminary lifecycle cost analysis suggests that the upfront investment is recouped within a few years through avoided premature failures.

Concerning the specificity of our findings to the Persian Gulf coast, it is important to note that the FEM simulations were performed using generic mechanical inputs (wind speed of 20 m/s, soil elasticity moduli of 1000 and 10000 ksi, standard concrete properties) and are not inherently calibrated to the specific conditions of this region. However, the corrosive environment of the Persian Gulf coast is exceptionally aggressive due to high concentrations of airborne chlorides and sulfates, elevated temperatures, and humidity. Under such hostile conditions, reducing mechanical shear—an accelerating factor for corrosion—becomes critically necessary. For other geographic regions with milder corrosive environments or different wind regimes (e.g., lower wind speeds, different gust spectra) or soil conditions (e.g., higher or lower foundation elasticity), the optimal parameters—such as span length, pole strength, or backfill type—may require re-calibration. The proposed methodology remains valid, but local wind data, soil properties, and corrosion risk levels should inform region-specific adjustments.

Based on our findings, we propose the following specific modifications to the relevant Iranian national standards for MV overhead lines in coastal corrosive regions: (1) prohibition of concrete backfill, mandating only compacted soil backfill; (2) prohibition of pin-type insulators, requiring suspension insulators exclusively; (3) mandatory symmetric conductor arrangements (i.e., no L-type, flag, or tangential configurations); (4) maximum span length of 40 m; and (5) exclusive use of 9 m or 12 m poles instead of the currently common 14 m and 15 m poles. Regarding safety risks, the primary concern is reduced ground clearance when using shorter poles, particularly 9 m poles. However, this risk is acceptable in the majority of suburban and rural applications, especially when conductors with XLPE insulation are employed. For urban areas or locations with higher safety requirements, 12 m poles represent a safer compromise while still providing substantial stress reduction compared to 14 m or 15 m designs.

Alternative mitigation strategies such as advanced concrete coatings, cathodic protection systems, or alternative pole materials (e.g., steel-reinforced polymer composites, fiber-reinforced concrete) were not within the scope of this work. These approaches hold promise and may act synergistically with our proposed modifications. Therefore, we recommend comparative evaluation of these strategies as a valuable direction for future research. Additionally, while long-term validation of the proposed service life extension would ideally require dedicated experimental research such as accelerated corrosion-fatigue testing on full-scale or segmented poles under controlled laboratory conditions, it is worth noting that the Hormozgan Electric Distribution Company (HEDC) is currently conducting ongoing research on a complementary topic: the development of a non-destructive device for estimating the corrosion level of embedded steel armor inside in-service concrete poles. This effort will provide valuable long-term field data on pole degradation rates. Future systematic corrosion-fatigue experiments—including cyclic mechanical loading combined with accelerated chloride/sulfate exposure—are recommended to quantitatively establish the relationship between shear stress reduction and service life extension.

8. Conclusion

In this article, the effective factors for stress reduction on the concrete poles of MV lines were investigated. It was observed that reducing the length of the cross arm (L-arm), reducing the length of the pole, suspending the conductors (corresponding insulators), reducing the number of MV circuits on the pole, reducing the strength of the base (the volume of the concrete structure) and increasing the elasticity of backfill (soil instead of concrete backfill for example) can all have a direct effect on reducing the pressure on the pole anchor. This reduced mechanical stress can significantly decrease the cracks and porosity of the concrete against corrosive agents and unnecessary large costs.

9. Acknowledgment

The authors would like to thank the Research Working Group at HEDC, especially Dr. Abdollah Ranjbar and Sadegh Sabouri, for their assistance at different stages of this project.

10. Fund

This work was supported by the Hormozgan Electric Distribution Company (HEDC) under Grant No. 140082.

11. References

1. M. Maslehuddin, "Concrete durability – The Gulf experience," in *Proc. Symp. Civil Engineering and the Environment*, King Fahd Univ., Saudi Arabia, May 3–5, 1997, pp. 1–12.
2. M. Haque, H. Al-Khaiat, and B. John, "Proposals for a draft code for designing durable concrete structures in the Gulf," *Arab. J. Sci. Eng.*, vol. 31, no. 1, Jun. 2006.
3. M. Mazloom, A. A. Ramezanianpour, and J. J. Brooks, "Effect of silica fume on mechanical properties of high-strength concrete," *Cem. Concr. Compos.*, vol. 26, pp. 347–357, 2004.
4. A. Aghajani et al., "Stray alternating current problems in concrete power poles," *Mater. Perform.*, vol. 52, no. 5, May 2013.
5. M. Zargar, H. Gholami, M. Ghane, K. Ostad-Ali-Askari, and V. P. Singh, "Mechanical view of corrosion phenomenon in concrete quadrangular of power transmission lines," *Int. J. Mod. Stud. Mech. Eng. (IJMSME)*, vol. 5, no. 2, pp. 30–43, 2019, doi: 10.20431/2454-9711.0502004.
6. K. SivaPrasad, "Analysis of stresses in tapered rectangular utility pole," *Int. J. Adv. Des. Manuf. Technol.*, vol. 11, no. 1, Mar. 2018.

7. S. A. Mundhada and A. R. Mundhada, "Comparative study of pre-tensioned pre-stressed concrete electric poles of Type I, II & III," *Int. J. Emerg. Technol. Adv. Eng.*, vol. 3, no. 12, pp. 594–598, 2013.
8. M. Zeynalian and M. Zamani Khorasgani, "Structural performance of concrete poles used in electric power distribution network," *Arch. Civ. Mech. Eng.*, vol. 18, no. 3, pp. 863–876, 2018, doi: 10.1016/j.acme.2018.01.005.
9. X. Li, Y.-S. Liang, Z.-H. Zhao, and H.-L. Lv, "Low-cycle fatigue behavior of corroded and CFRP-wrapped reinforced concrete columns," *Constr. Build. Mater.*, vol. 101, pt. 1, pp. 902–917, 2015, doi: 10.1016/j.conbuildmat.2015.10.063.
10. International Electrotechnical Commission (IEC), *Insulators for overhead lines – Composite suspension and tension insulators*, IEC 61109, 3rd ed., Geneva, Switzerland, 2025.
11. M. S. Amouri and N. M. Fawzi, "Mechanistic insights into the long-term sulphate–chloride co-exposure resistance of self-compacting engineered cementitious composites," *Civil Environ. Eng.*, vol. 22, no. 1, 2026.
12. M. J. Brown, C. Davidson, C. J. Shepherd, S. M. Flint, and S. Mbisike, "Sustainable overhead line equipment foundations with optimised shape and backfilling," *Proc. Inst. Civ. Eng. Geotech. Eng.*, 2026.
13. Y. Song, Y. Wang, Y. Wang, and B. Liu, "Chloride-induced rebar corrosion behavior in concrete within and above water level fluctuating zone under sulfate attack," *Constr. Build. Mater.*, vol. 458, 2025.

Appendix

Table 4. Conductor (insulator pin) coordinate x,y in cm – take pole tip (0,0)

Arrange	R1	S1	T1	R2	S2	T2
A-types	(x,-14)	(x,-104)	(x,-204)	(-x,-14)	(-x,-104)	(-x,-204)
B-types	(x,-14)	(x,-104)	(x,-204)	(-x,-14)	(-x,-104)	(-x,-204)
C-types	(x,-14)	(x,-104)	(x,-204)	(-x,-14)	(-x,-104)	(-x,-204)
D-type	(55,-44)	(125,-44)	(195,-44)	-	-	-
E-type	(-112,-14)	(48,-14)	(112,-14)	-	-	-
F-type	(60,-14)	(60,-104)	(60,-204)	-	-	-
G-types	(-70,-110)	(0,-14)	(-70,110)	-	-	-

Table. 5. Tip and base dimensions (cm×cm) of the poles referring to fig 12

Pole Strength	A1	A2	A3	A4
400 kgf	19×22	31×46	36×54	38×56
600 kgf	19×25	37×55	42×63	44×64

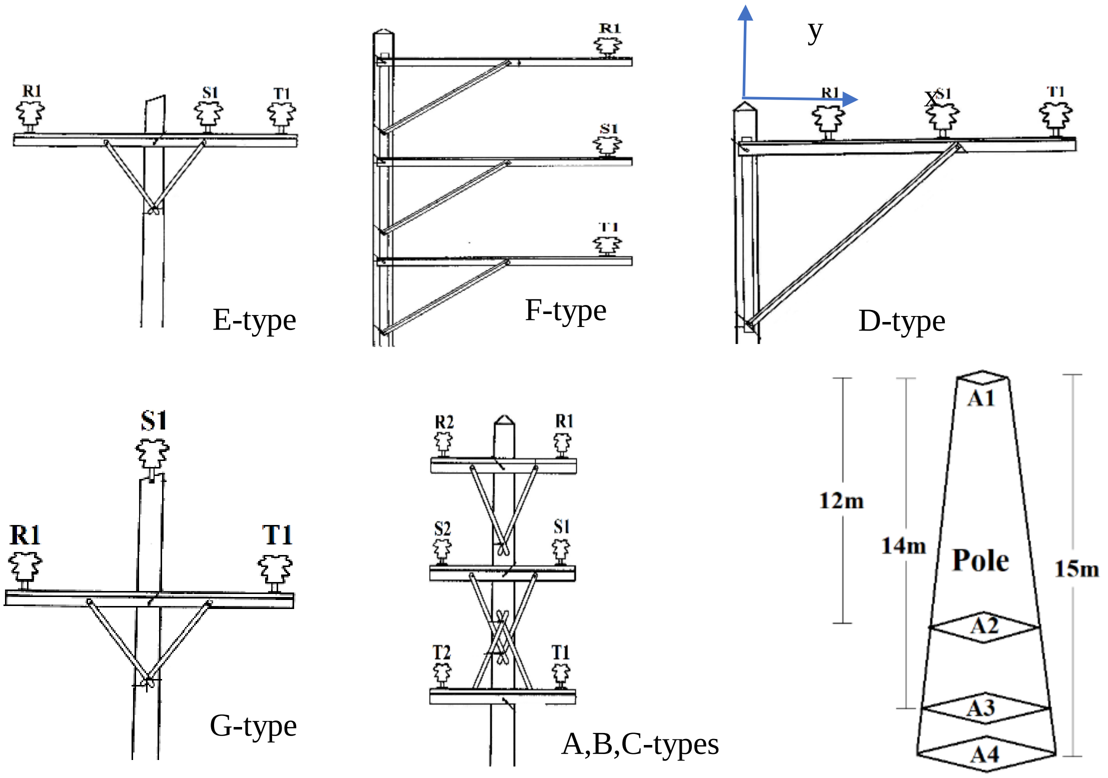

Fig. 12. Common arrangements of medium pressure lines of Hormozgan Electricity Distribution Company